AJNR

Monitoring Peri-Therapeutic Cerebral Circulation Time: A Feasibility Study Using Color-Coded Quantitative DSA in Patients with Steno-Occlusive Arterial Disease

C.J. Lin, S.C. Hung, W.Y. Guo, F.C. Chang, C.B. Luo, J. Beilner, M. Kowarschik, W.F. Chu and C.Y. Chang

AJNR Am J Neuroradiol published online 12 April 2012
http://www.ajnr.org/content/early/2012/04/12/ajnr.A3049

Published April 12, 2012 as 10.3174/ajnr.A3049

Monitoring Peri-Therapeutic Cerebral Circulation Time: A Feasibility Study Using Color-Coded Quantitative DSA in Patients with Steno-Occlusive Arterial Disease

ORIGINAL RESEARCH

C.J. Lin
S.C. Hung
W.Y. Guo
F.C. Chang
C.B. Luo
J. Beilner
M. Kowarschik
W.F. Chu
C.Y. Chang

BACKGROUND AND PURPOSE: Intracranial hemodynamics are important for management of SOAD. This study aimed to monitor peri-stent placement intracranial CirT of patients with SOAD.

MATERIALS AND METHODS: Twenty-five patients received stent placement for extracranial ICA stenosis, and 34 patients with normal CirT were recruited as controls. Their color-coded DSAs were used to define the Tmax of selected intravascular ROI. A total of 20 ROIs of the ICA, OphA, ACA, MCA, FV, PV, OV, SSS, SS, IJV, and MCV were selected. rTmax was defined as the Tmax at the selected region of interest minus Tmax at the cervical segment of the ICA (I1 on AP view and IA on lateral view). rTmax of the PV was defined as intracranial CirT. Intergroup and intragroup longitudinal comparisons of rTmax were performed.

RESULTS: rTmax values of the normal cohorts were as follows: ICA-AP, 0.12; ICA-LAT, 0.10; A1, 0.28; A2, 0.53; A3, 0.81; M1, 0.40; M2, 0.80; M3, 0.95; OphA, 0.35; FV, 4.83; PV, 5.11; OV, 5.17; SSS, 6.16; SS, 6.51; IJV, 6.81; and MCV, 3.86 seconds. Before stent placement, the rTmax values of arterial ROIs, except A3 and M3, were prolonged compared with values from control subjects ($P < .05$). None of the rTmax of any venous ROIs in the stenotic group was prolonged with significance. After stent placement, the rTmax of all arterial ROIs shortened significantly, except A1and M3. Poststenting rTmax was not different from the control group.

CONCLUSIONS: Without extra contrast medium and radiation dosages, color-coded quantitative DSA enables real-time monitoring of peri-therapeutic intracranial CirT in patients with SOAD.

ABBREVIATIONS: AP = anterior-posterior view; AUC = area under the ROC curve; CI = confidence interval; CirT = circulation time; FV = cortical veins at the frontal region; ICA-AP = internal carotid artery on anterior-posterior view; ICA-LAT = internal carotid artery on lateral view; ICC = intraclass correlation coefficient; IJV = internal jugular vein; MCV = middle cerebral vein; OphA = ophthalmic artery; OV = cortical veins at occipital region; PV = cortical veins at parietal region; rTmax = relative Tmax; ROC = receiver operating characteristic; SOAD = steno-occlusive arterial disease; SS = sigmoid sinus; SSS = superior sagittal sinus; Tmax = time to maximum opacification

Cerebral angiography, using the attenuation effects of x-ray radiation caused by intravascular administration of a contrast agent, has been the reference standard for studying neurovascular disorders for approximately 80 years.[1,2] DSA's spatial and temporal resolutions are superior to those of CT angiography using multidetector CT and 3D time-resolved MR angiography.[3-6] Nevertheless, quantitative measurements of blood flow using DSA rarely have been explored.[7-9] Recently, Strother et al suggested the color-coded parametric method for illustrating the Tmax of intracranial arteriovenous malformations.[10] The composite DSA imaging increases the conspicuity of subtle changes in blood flow over what could be seen previously by looking at sequential timeframes. It also makes real-time evaluation of intracranial CirT feasible. In clinical practice, monitoring treatment effects for early prediction of therapeutic outcomes is the trend of modern medical care.[11] Examples from recent studies demonstrated the feasibility of using flat panel DSA to study parenchymal blood volume of brain and estimate the infarction core in patients with acute ischemic insults.[12,13] Similarly, using DSA, we hypothesized that intracranial CirT can serve as a "hemodynamic marker" in those patients with carotid stenosis. With the "marker," in-room and real-time assessment of the therapeutic effects of stent placement could be feasible. Therefore, we conducted the current study to 1) measure the intracranial CirT on DSA, 2) compare the CirT of patients with SOAD with that of control subjects, and 3) longitudinally monitor the peri-therapeutic CirT relevant to stent placement.

Received November 8, 2011; accepted after revision January 2, 2012.

From the Department of Radiology (C.J.L., S.C.H., W.Y.G., F.C.C., C.B.L., W.F.C., C.Y.C.), Taipei Veterans General Hospital, Taipei, Taiwan; School of Medicine (C.J.L., S.C.H., W.Y.G., F.C.C., C.B.L., C.Y.C.), National Yang-Ming University, Taipei, Taiwan; Siemens Ltd. China, Healthcare Sector (J.B.), Angiography & Interventional X-Ray Systems, Shanghai, P.R. China; Siemens AG, Healthcare Sector (M.K.), Angiography & Interventional X-Ray Systems, Forchheim, Germany.

This research is cosponsored by Taipei Veterans General Hospital and Siemens Healthcare (grant number: T1100200).

This work, in part, was presented as a scientific format paper at the annual meeting of the Radiological Society of North America, November 27–December 2, 2011; Chicago, Illinois.

Please address correspondence to Wan-Yuo Guo, MD, PhD, Department of Radiology, Taipei Veterans General Hospital, No. 201, Sec. II, Shipai Road, Taipei, 11217, Taiwan; e-mail: wyguo@vghtpe.gov.tw

http://dx.doi.org/10.3174/ajnr.A3049

Methods

Patient Selection

The institutional review board approved this study. Informed consent was obtained before conducting DSA. From March to May 2011, 29

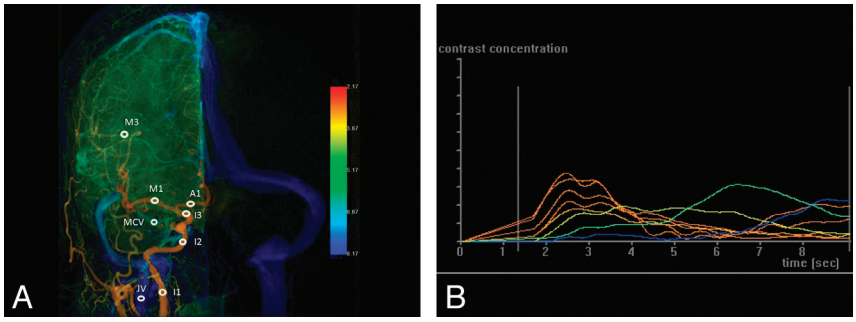

Fig 1. *A*, AP view of color-coded right carotid artery DSA of a control subject. Arterial region of interest: I1, cervical portion of ICA; I2, cavernous portion of ICA; I3, supraclinoid portion of ICA; A1, the midpoint of the first portion of ACA; M1, the midpoint of the first segment of MCA; and M3, the point immediately after the turning junction of the second and third segment of MCA. The venous region of interest: IJV is located at a point 2 cm below its junction with SS, and MCV at the midpoint of the ascending limb of MCV. *B*, Time-attenuation curves of the 8 ROIs on AP view (horizontal axis: imaging timeline of DSA in sec; vertical axis: contrast medium opacification). The time point of maximum contrast medium opacification of each curve is defined as the Tmax of each region of interest.

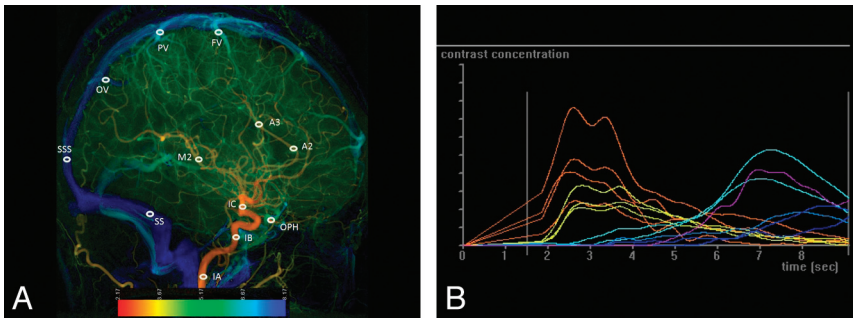

Fig 2. *A*, Lateral view of a color-coded right carotid artery DSA of a control subject. Arterial region of interest: IA, cervical portion of ICA; IB, cavernous portion of ICA; IC, supraclinoid portion of ICA; A2, the midpoint of the second portion of ACA; A3, a point in the proximal segment of pericallosal artery; and M2, a point in the proximal temporal branch of MCA before its bifurcation. The venous region of interest of FV, PV, and OV are designated at just before their entry to SSS; SSS, a point located 2 cm above the torcular herophili; SS, the midpoint of sigmoid sinus. *B*, Time-attenuation curves of the 12 ROIs on lateral view.

patients with imaging-confirmed extracranial carotid artery stenosis ≥70%, according to NASCET criteria, were referred to our department for stent placement treatment. Two subjects with underlying heart disease and 2 subjects with suboptimal imaging quality, caused by motion artifacts, were excluded. A total of 25 patients with 25 DSAs were available for analysis (mean age 73.8 years; 23 men and 2 women). We enrolled another 34 patients (mean age 64.6 years; 24 men and 10 women) with no conceivable intracranial circulatory disturbance as the control group during the same period. These patients were initially referred for DSA under the clinical suspicion of other intracranial diseases that do not affect intracranial circulation.

Imaging Protocol and Data Analysis

A 4F angiocatheter was placed at the level of the C4 vertebral body for DSA. The imaging parameters were 6 frames per second for 12 seconds with 12 mL of a 60% diluted contrast medium (340 mgI/mL) for all series in all subjects. Each patient's pretreatment angiogram was used as the reference to ensure the same projections in posttreatment angiography. Throughout the procedure, the patient's head was fixed to the angiography suite table by a plastic band. The contrast medium was administered for 1.5 seconds using a power injector (Liebel-Flarsheim Angiomat Illumena; Cincinnati, Ohio). The same biplane angiography suite (Axiom-Artis; Siemens, Erlangen, Germany) was used for all DSA throughout the study. All angiography acquisition was tailored for clinical diagnosis without additional series. Postprocessing software (syngo iFlow; Siemens) was used to color-code the DSA, according to the time to Tmax in seconds.[10] The Tmax of any selected region of interest on DSA was defined as the time point when the attenuation of the x-ray reached its maximum along the angiographic frames. The diameter of a region of interest was the caliber of a selected vessel. The reference time point, $t = 0$, was defined as the imaging time of the selected mask of the angiographic frames. Eight ROIs on AP (Fig 1*A*, -*B*) and 12 ROIs on lateral (Fig 2*A*, -*B*) views of DSA were defined. The Tmax values of ICA-AP and ICA-LAT were defined as the average of 3 ROIs located at the cervical, cavernous, and supraclinoid portions of the ICA on AP (I1, I2, I3) and lateral views (IA, IB, IC), respectively. When an intended region of interest demonstrated laminated heterogeneous attenuation, we repositioned the region of interest at an upstream or downstream vascular segment in the vicinity that contained homogeneous attenuation. The heterogeneous attenuation was usually caused by confluent flows from a mixture of noniodinated and iodinated blood, such as the A1 segment of the ACA with confluent flows from the contralateral ACA via the anterior communicating artery. The placement of a region of interest for measuring Tmax among the 59 total patients was conducted independently by 2 neuroradiologists. They were not aware of the degree of arterial stenosis of the patients. Tmax values were defined as the average of 2 sets of the measurement. To normalize the intracranial CirT, Greitz used the time difference between the points of maximum concentration in the carotid siphon and in the parietal veins as the circulation time.[14] We adopted this method and defined rTmax as Tmax at any selected region of interest minus the Tmax of I1 on AP view or Tmax of IA on lateral view DSA. Hence, the CirT in the current study was defined as the rTmax of cortical veins at parietal minus rTmax at I1 on AP view or IA on lateral view DSA.

Table 1: Interobserver reliability of rTmax measurements at different ROIs

ROI	ICC (95% CI)
AP view	
ICA-AP	0.680 (0.408, 0.841)
A1	0.620 (0.169, 0.856)
M1	0.560 (0.232, 0.773)
M3	0.580 (0.260, 0.785)
MCV	0.320 (0.086, 0.542)
JV	0.310 (−0.084, 0.620)
Lateral view	
ICA-LAT	0.410 (0.040, 0.681)
OphA	0.610 (0.295, 0.805)
A2	0.430 (0.186, 0.639)
A3	0.460 (−0.216, 0.838)
M2	0.460 (0.101, 0.713)
FV	0.22 (−0.295, 0.466)
PV	0.480 (−0.192, 0.846)
OV	0.310 (0.108, 0.391)
SSS	0.330 (−0.178, 0.665)
SS	0.320 (−0.073, 0.627)

Statistical Analysis

All statistical analyses were performed using SAS 9.2 (SAS Institute, Cary, North Carolina). The ICC with 95% CI was calculated to assess the interobserver reliability of rTmax measurements. ICC values were compared with the following scale: almost perfect (1.00–0.8), substantial (0.8–0.6), moderate (0.6–0.4), fair (0.4–0.2), and slight (<0.2). If the 95% CI of ICC covers zero, it indicates no significant correlation in rTmax measurement between 2 neuroradiologists (Table 1). The CirT difference between the stenotic and control groups was examined using a Student *t* test. The longitudinal changes of CirT along the stent placement were examined using a paired *t* test. Significance was set to $P = .05$.

Results

The rTmax measurements at arterial ROIs showed substantial to moderate agreement between 2 neuroradiologists (ICC ranged from 0.68–0.52), except A2 showed slight agreement (ICC = 0.21; 95% CIs, −0.21, 0.52). All the venous ROIs showed fair agreement (ICC ranged from 0.31–0.33) except PV showed moderate agreement (ICC = 0.46; 95% CIs, −0.19, 0.85) (Table 1). The normal intracranial CirTs of the control group were 5.11 ± 1.00 seconds, which were similar to those reported by Greitz[14] (4.67 ± 1.08 seconds). The mean rTmax values of all ROIs in the control and prestenting patient groups are listed in Table 2. Before stent placement, all rTmax values of the ICA, ACA, and MCA ROIs on the AP view were significantly prolonged, except M3 ($P = .12$); all rTmax values of the ICA, ACA, and MCA ROIs on the lateral view were prolonged with significance, except A3 ($P = .06$), indicating prolonged CirT. None of the venous ROIs prolonged with significance. The ROC curves for those 7 ROIs (ICA-AP, A1, M1, ICA-LAT, OphA, A2, and M2) showing significantly different rTmax values are displayed in Fig 3. The AUC showed the highest discriminatory power to distinguish patients from controls using rTmax at OphA (AUC = 0.890; 95% CIs, 0.802, 0.977), with optimal cutoff value in rTmax of 0.670 as an upper limit to detect patients with carotid stenosis; the sensitivity and specificity were 66.7% and 91.2%, respectively (Table 3). The second highest AUC was observed at M1 (AUC = 0.759; 95% CIs, 0.627, 0.891), with optimal cutoff value in rTmax of 0.340; the sensitivity and specificity were 94.4% and 50.0%, respectively. The rTmax of MCV was always shorter than that of all veins on the convexity (3.86 versus 5.04 seconds; $P < .05$). The rTmax values of cortical veins tended to be shorter in the frontal region and followed by the parietal and occipital regions, though the difference was not significant.

Table 2: Comparison of the average rTmax of each ROI in patients with carotid stenosis versus the control group

	Patient Group (Prestenting, $n = 25$)	Control Group ($n = 34$)	*P* Value
AP view			
ICA-AP	0.35 ± 0.31	0.12 ± 0.11	0.01*
A1	0.54 ± 0.39 ($n = 15$)	0.28 ± 0.28	0.01*
M1	0.72 ± 0.41	0.40 ± 0.32	$P < 0.001$*
M3	1.05 ± 0.41	0.80 ± 0.37	0.12
MCV	3.79 ± 2.04	3.86 ± 1.70	0.23
IJV	6.83 ± 1.11	6.81 ± 1.25	0.45
Lateral view			
ICA-LAT	0.23 ± 0.25	0.10 ± 0.11	0.002*
OphA	0.97 ± 0.67	0.35 ± 0.22	$P < 0.001$*
A2	0.86 ± 0.68 ($n = 15$)	0.53 ± 0.35	0.01*
A3	1.03 ± 0.62 ($n = 15$)	0.81 ± 0.40	0.06
M2	1.31 ± 0.59	0.95 ± 0.36	0.002*
FV	5.12 ± 1.4	4.83 ± 0.93	0.17
PV	5.41 ± 0.87	5.11 ± 1.00	0.35
OV	5.36 ± 1.41	5.17 ± 1.01	0.27
SSS	6.28 ± 1.60	6.16 ± 1.14	0.37
SS	6.64 ± 1.56	6.51 ± 1.10	0.4

* Statistically significant ($P < .05$).

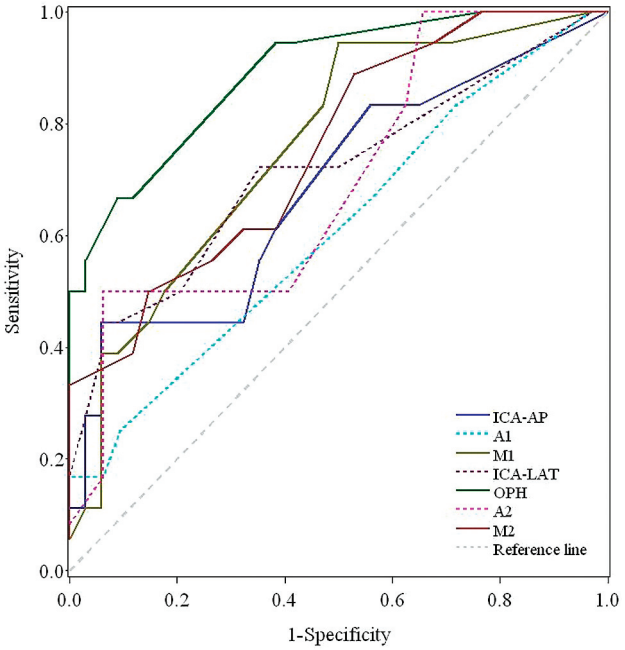

Fig 3. The ROC curves of rTmax values at 7 different arterial ROIs.

The peri-procedural comparison of rTmax values of all ROIs along the stent placement is listed in Table 4. After stent placement, all Tmax values of the arterial region of interest were shortened with significance, except A1, A3, and M3. Before stent placement, the flow in the distal runoff of ACA was not detectable in 15 of 25 patients, presumably because of

Table 3: Diagnostic performance of rTmax at 7 ROIs

ROI	AUC (95%CI)	*P* value	Optimal Cutoff Value	Sensitivity	Specificity	PPV	NPV
ICA-AP	0.686 (0.527–0.844)	0.021	0.340	44.4%	94.1%	80.0%	76.2%
A1	0.609 (0.417–0.802)	0.260	0.840	16.7%	100.0%	100.0%	76.2%
M1	0.759 (0.627–0.891)	0.0001	0.340	94.4%	50.0%	50.0%	94.4%
ICA-LAT	0.716 (0.561–0.870)	0.006	0.267	44.4%	94.1%	80.0%	76.2%
OphA	0.890 (0.802–0.977)	<.0001	0.670	66.7%	91.2%	80.0%	83.8%
A2	0.698 (0.520–0.876)	0.030	1.000	50.0%	93.8%	75.0%	83.3%
M2	0.754 (0.617–0.891)	0.0003	0.840	88.9%	47.1%	47.1%	88.9%

Note.—NPV, negative predictive value; PPV, positive predictive value.

Table 4: Comparison of the average rTmax of each ROI in patients with carotid stenosis before and after stenting

	Before Stenting ($n = 25$)	After Stenting ($n = 25$)	*P* Value
AP view			
ICA-AP	0.35 ± 0.31	0.17 ± 0.22	0.002*
A1	0.54 ± 0.39 (n = 15)	0.49 ± 0.44	0.28
M1	0.72 ± 0.41	0.53 ± 0.39	0.01*
M3	1.05 ± 0.41	1.18 ± 1.58	0.33
IJV	6.83 ± 1.11	6.58 ± 1.35	0.38
MCV	3.79 ± 2.04	3.75 ± 1.50	0.47
Lateral view			
ICA-LAT	0.23 ± 0.25	0.11 ± 0.15	0.01*
OphA	0.97 ± 0.67	0.54 ± 0.54	0.01*
A2	0.86 ± 0.68 (n = 15)	0.53 ± 0.48	0.01*
A3	1.03 ± 0.62 (n = 15)	0.84 ± 0.50	0.02*
M2	1.31 ± 0.59	1.07 ± 0.55	0.03*
FV	5.12 ± 1.4	4.84 ± 1.25	0.22
PV	5.41 ± 0.87	4.89 ± 1.28	0.18
OV	5.36 ± 1.41	4.88 ± 1.21	0.11
SSS	6.28 ± 1.60	6.04 ± 2.12	0.31
SS	6.64 ± 1.56	6.25 ± 2.10	0.40

* Statistically significant ($p < 0.05$).

severe stenosis. In 7 of the 10, the flow was reconstituted after stent placement (Fig 4*A–D*). The other 3 remained undetectable and were considered as cases of A1 aplasia. Before stent placement, the rTmax of OphA in the stenotic group was prolonged compared with that of the control group ($P < .001$). After stent placement, the rTmax of OphA reduced, but not significantly. As a group, poststenting rTmax was normalized and not different from the control group.

Discussion

The current study has shown the ability of color-coded DSA to visualize and quantitatively define the differences and changes in blood flow during stent placement procedures in patients with SOAD. Although the size of the control cohort is small, the results of normal intracranial CirT may be used as a reference for initial comparison. A larger scale of cohort size should be enlisted for in a future study. The intracranial CirT of patients with SOAD is longer than the control cohort, with significance. The variation of rTmax of patients is wider compared with those in the control group. The wide variation may stem from the arterial stenosis and blunt peak of Tmax. After stent placement in the steno-occlusive ICA, the intracranial CirT is normalized and not different from the control cohort. The data were all processed after the completion of DSA acquisition and thus did not increase the radiation and contrast-medium dosages at all. Moreover, the postprocessing can feasibly be conducted in the angiography suite with almost no time delay. The imaging strategy may help to refine the interventional procedure before the patient leaves the angiography suite after the endovascular treatment.

Several other methods are available for analyzing flow based on time-attenuation curves, such as mathematical cross-sectional computation, shifted distance-attenuation curves, and gamma-variate fitting.[8,15,16] These methods are computationally intensive and are still constrained by the 2D imaging nature of DSA. One of the major limitations and uncontrollable variations in studying flow in vivo has been the individualized cardiac output. This phenomenon is, however, less prominent in intracranial circulation due to autoregulation.[17,18] We further minimized this effect by excluding those patients with congestive heart failure. Moreover, because of the laminated and turbulent properties of flow propagation in vessels in vivo, flows in vessels are not always homogeneous both temporally and spatially. These flow patterns may explain the variances in the measurement of rTmax. The use of the region of interest of a selected vessel may minimize the inhomogeneity.

Various definitions of intracranial CirT, ranging from 4–12 seconds, have been proposed.[1,2,19] We used the CirT according to the method proposed by Greitz because it consists of the lowest systemic error and provides high reproducibility between different observers and patient populations.[14] Furthermore, Greitz proved that the CirT defined on x-ray angiography was correlated linearly to CBF. The linearity disappeared when CBF was significantly decreased. Therefore, he concluded that x-ray angiography was more sensitive in detecting the decreased flow that occurred in patients with SOAD compared with the diffusible isotope technique.[8,20,21] Recent correlation of CT perfusion and DSA also demonstrate similar findings.[22] Both studies proved that CirT provides reliable information on cerebral blood flow.

The prestenting time-attenuation curves are shallower and

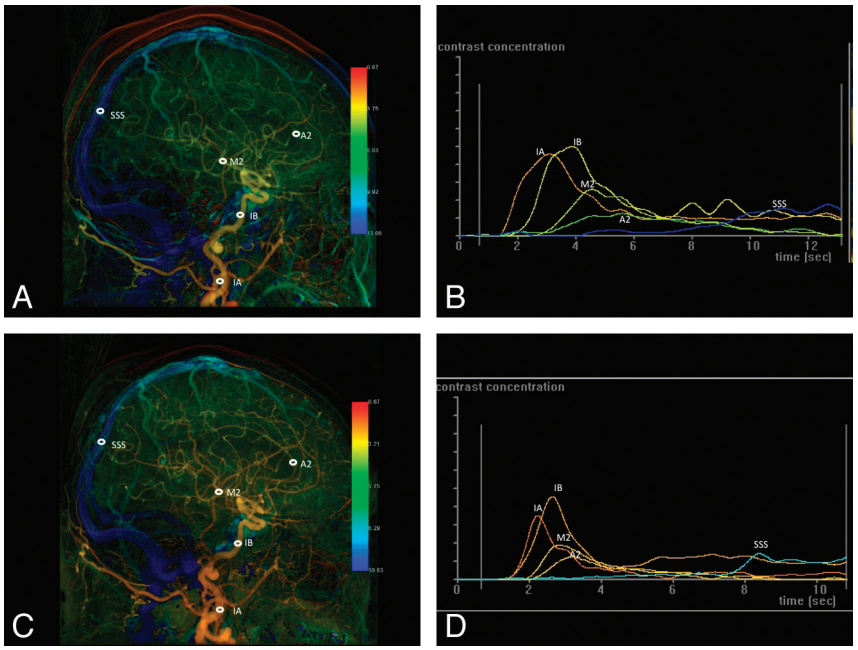

Fig 4. *A*, Lateral view of color-coded left carotid artery DSA of a 78-year-old man with 90% stenosis of the left proximal ICA. Before stent placement, 5 ROIs were selected in the following order: cervical portion of ICA (IA), cavernous portion of ICA (IB), the second portion of ACA (A2), the temporal branch of MCA (M2), and SSS. *B*, Time-attenuation curves of the selected ROIs in *A*. *C*, Lateral view of the color-coded left carotid artery DSA of the same patient after stent placement. The same 5 selected ROIs as in *A*. *D*, After stent placement, the time-attenuation curves of the arterial ROIs become steeper and their Tmax values shorter, whereas no interval change of the waveform of SSS is evident compared with the corresponding waveform before stent placement in *B*.

broader compared with those after stent placement (Fig 4). Delayed and dispersed contrast medium bolus, with probable turbulences caused by arterial stenosis, explains the involved waveform changes. This phenomenon is consistent with that observed in Doppler sonography of poststenotic vessels.[23] Moreover, this phenomenon is more evident at the ICA than at its distal arterial runoffs and veins.

The Tmax measurement is complicated by the confluent flows that stemmed from the circle of Willis. The specific intracranial collateral circulation system makes the MCA a more reliable "hemodynamic marker" than ACA in SOAD. Another typical example is the collateral circulation via OphA. In patients with severe ICA stenosis, OphA may be irrigated retrospectively via the infraorbital branches of the distal internal maxillary artery. Thus, the Tmax measurement adds value to DSA by determining the flow direction of OphA illustrated by its CirT.

Although global prolongation of venous rTmax was observed in SOAD, the prolongation was not directly related to the arterial territories. For example, OV drains both the temporo-occipital branches of the MCA and the calcarine branch of the PCA; thus, their rTmax values were not significantly prolonged.

There are some other limitations. First, because of the large gap between the caliber of angiocatheters and examined arteries, usually the CCA, the injected contrast medium is diluted by continuous mixing with noniodinated blood. This produces multiple fluctuating ascending and declining contrast-medium peaks along the time-attenuation curves and complicates the Tmax determination. Further investigation of the rhythmic changes of velocities during cardiac cycles, and the advantages of using a power injector that simulates cardiac output, may warrant improvement to the algorithms. In addition, CirT may vary according to the total amount and duration of contrast-medium administration and positioning of angiographic catheters, and even patient positioning during imaging acquisition. All of these factors may change the bolus shape of contrast-medium propagation in the examined vessels and may subsequently influence the measurement of Tmax.[14] In the current study, these factors were, for the most part, standardized. Furthermore, we used rTmax to address the variability of contrast traveling time between the heart and cervical ICA. Second, the regional concentration of a contrast medium will be diluted due to collateral flows via the circle of Willis and lead to misinterpretation of Tmax, particularly in the ACA. Third, DSA is basically 2D imaging. Overlapping and collapsing all vasculatures on a 2D projection, for example, the cavernous portion of the ICA on the AP view and the proximal MCA on lateral view, can accentuate the contrast-medium attenuation and mistakenly shift the Tmax. Recent advances in flat panel detector technology, combined with a rotational C-arm for generating rotational angiography, have provided a novel method for overcoming the constraints of 2-dimensionality.[24-27] In addition, coregistration with other 3D imaging may further facilitate the feasibility of flow analysis in the future.[28,29]

Conclusion

This study established the reference of normal intracranial CirT and confirmed the feasibility of monitoring the therapeutic effects of stent placement procedures in patients with extracranial SOAD. Without additional burdens of contrast medium and radiation exposure, color-coded DSA improves the ability to visualize differences and quantitative changes in blood flow, in-room and in real-time, which may help the management of intracranial vascular diseases.

Disclosures: Janina Beilner—*UNRELATED: Employment:* Siemens Healthcare, Comments: I am employed by Siemens Healthcare. Siemens Healthcare supports some of the scientific activities on which this manuscript is based. The research that is presented in this manuscript relates to an application of the Siemens software product syngo iFlow. Markus Kowarschik—*UNRELATED: Employment:* Siemens Healthcare, Comments: I am employed by Siemens Healthcare. Siemens Healthcare supports some of the scientific activities on which this manuscript is based.

Acknowledgments

We would like to thank Eric C.S. Lin for his assistance with the statistical analysis.

References

1. Raney R, Raney AA, Sanchez-Perez JM. **The role of complete cerebral angiography in neurosurgery.** *J Neurosurg* 1949;6:222–37
2. Curtis JB. **Rapid serial angiography; preliminary report.** *J Neurol Neurosurg Psychiatr* 1949;12:167–81
3. Luo Z, Wang D, Sun X, et al. **Comparison of the accuracy of subtraction CT angiography performed on 320-detector row volume CT with conventional CT angiography for diagnosis of intracranial aneurysms.** *Eur J Radiol* 2011;81:118–22
4. Roth C. **Value of CT and MR angiography for diagnostics of intracranial aneurysms.** *Radiologe* 2011;51:106–12
5. Petkova M, Gauvrit J-Y, Trystram D, et al. **Three-dimensional dynamic time-resolved contrast-enhanced MRA using parallel imaging and a variable rate k-space sampling strategy in intracranial arteriovenous malformations.** *J Magn Reson Imaging* 2009;29:7–12
6. Lee Y-J, Laub G, Jung S-L, et al. **Low-dose 3D time-resolved magnetic resonance angiography (MRA) of the supraaortic arteries: correlation with high spatial resolution 3D contrast-enhanced MRA.** *J Magn Reson Imaging* 2011;33:71–76
7. Dobben GD, Valvassori GE, Mafee MF, et al. **Evaluation of brain circulation by rapid rotational computed tomography.** *Radiology* 1979;133:105–11
8. Kruger RA, Bateman W, Liu PY, et al. **Blood flow determination using recursive processing: a digital radiographic method.** *Radiology* 1983;149:293–98
9. Westermark N. **Studies of the circulation by roentgencinematography.** *Radiology* 1948;50:791–802
10. Strother CM, Bender F, Deuerling-Zheng Y, et al. **Parametric color coding of digital subtraction angiography.** *AJNR Am J Neuroradiol* 2010;31:919–24
11. Hamstra DA, Chenevert TL, Moffat BA, et al. **Evaluation of the functional diffusion map as an early biomarker of time-to-progression and overall survival in high-grade glioma.** *Proc Natl Acad Sci U S A* 2005;102:16759–64
12. Struffert T, Deuerling-Zheng Y, Kloska S, et al. **Flat detector CT in the evaluation of brain parenchyma, intracranial vasculature, and cerebral blood volume: a pilot study in patients with acute symptoms of cerebral ischemia.** *AJNR Am J Neuroradiol* 2010;31:1462–69
13. Struffert T, Ott S, Adamek E, et al. **Flat-detector computed tomography in the assessment of intracranial stents: comparison with multi detector CT and conventional angiography in a new animal model.** *Eur Radiol* 2011;21:1779–87
14. Greitz T. **A radiologic study of the brain circulation by rapid serial angiography of the carotid artery.** *Acta Radiol Suppl* 1956;140:1–123
15. Smedby O, Högman N, Nilsson S, et al. **Flow disturbances in early femoral atherosclerosis–an in vivo study with digitized cineangiography.** *J Biomech* 1993;26:1105–15
16. Starmer CF, Clark DO. **Computer computations of cardiac output using the gamma function.** *J Appl Physiol* 1970;28:219–20
17. Hacein-Bey L, Nour R, Pile-Spellman J, et al. **Adaptive changes of autoregulation in chronic cerebral hypotension with arteriovenous malformations: an acetazolamide-enhanced single-photon emission CT study.** *AJNR Am J Neuroradiol* 1995;16:1865–74
18. Shpilfoygel SD, Close RA, Valentino DJ, et al. **X-ray videodensitometric methods for blood flow and velocity measurement: a critical review of literature.** *Med Phys* 2000;27:2008–23
19. Schurr PH, Wickbom I. **Rapid serial angiography: further experience.** *J Neurol Neurosurg Psychiatr* 1952;15:110–18
20. Yamamoto S, Watanabe M, Uematsu T, et al. **Correlation of angiographic circulation time and cerebrovascular reserve by acetazolamide-challenged single photon emission CT.** *AJNR Am J Neuroradiol* 2004;25:242–47
21. Gado M, Eichling J, Grubb R, et al. **Appraisal of the angiographic circulation time as an index of cerebral blood flow.** *Radiology* 1975;115:107–12
22. Aikawa H, Kazekawa K, Tsutsumi M, et al. **Intraprocedural changes in angiographic cerebral circulation time predict cerebral blood flow after carotid artery stenting.** *Neurol Med Chir (Tokyo)* 2010;50:269–74
23. Kamouchi M, Kishikawa K, Okada Y, et al. **Poststenotic flow and intracranial hemodynamics in patients with carotid stenosis: transoral carotid ultrasonography study.** *AJNR Am J Neuroradiol* 2005;26:76–81
24. Söderman M, Babic D, Holmin S, et al. **Brain imaging with a flat detector C-arm: technique and clinical interest of XperCT.** *Neuroradiology* 2008;50:863–68
25. Strobel N, Meissner O, Boese J, et al. **3D Imaging with flat-detector C-arm systems.** *In*; Reiser MF, Becker CR, Nikolaou K, Glazer G, eds. Multislice CT Part 1. Berlin: Springer; 2009:33–51
26. Hawkes DJ, Seifalian AM, Colchester AC, et al. **Validation of volume blood flow measurements using three-dimensional distance-concentration functions derived from digital x-ray angiograms.** *Invest Radiol* 1994;29:434–42
27. Heran N, Song J, Namba K, et al. **The utility of DynaCT in neuroendovascular procedures.** *AJNR Am J Neuroradiol* 2006;27:330–32
28. Lin C-J, Blanc R, Clarençon F, et al. **Overlying fluoroscopy and preacquired CT angiography for road-mapping in cerebral angiography.** *AJNR Am J Neuroradiol* 2010;31:494–95
29. Mistretta CA. **Sub-Nyquist acquisition and constrained reconstruction in time resolved angiography.** *Med Phys* 2011;38:2975–85